Scientific Research Publishing

American Journal of Plant Sciences, 2019, 10, 1949-1968
https://www.scirp.org/journal/ajps
ISSN Online: 2158-2750
ISSN Print: 2158-2742

Immunolocalization of a Normal Wood Specific Pectin Methylesterase (CoPME) and Quantification of PME Gene Expression in Differentiating Xylem of *Chamaecyparis obtusa*

Akinori Ota, Masato Yoshida*, Saori Sato, Hideto Hiraide, Miyuki Matsuo-Ueda, Hiroyuki Yamamoto

Graduate School of Bioagricultural Sciences, Laboratory of Wood Physics, Nagoya University, Nagoya, Japan
Email: *yoshida@agr.nagoya-u.ac.jp

How to cite this paper: Ota, A., Yoshida, M., Sato, S., Hiraide, H., Matsuo-Ueda, M. and Yamamoto, H. (2019) Immunolocalization of a Normal Wood Specific Pectin Methylesterase (CoPME) and Quantification of PME Gene Expression in Differentiating Xylem of *Chamaecyparis obtusa*. *American Journal of Plant Sciences*, **10**, 1949-1968.
https://doi.org/10.4236/ajps.2019.1011137

Received: October 9, 2019
Accepted: November 3, 2019
Published: November 6, 2019

Abstract

The transverse section of compression wood tracheids has a circular shape and intercellular spaces. The cause has not been determined yet; however, we hypothesized that peeling of the cell wall adhesion would cause cellular intervals, resulting in circularity of the transverse section of tracheids. Homogalacturonan, a type of pectin, functions in cell wall adhesion. Further, pectin methylesterase (PME) is involved in functionalization of homogalacturonan. We quantitated PME gene expression levels in differentiating xylem cells using different degrees of compression wood samples and examined the correlation with circularity of the transverse section of tracheids in each sample. We found that lower gene expression level of the sample corresponded with increasing circularity of the transverse section of tracheids. It is considered that the transverse section of compression wood tracheids becomes circular by suppression of PME gene expression during differentiation. Further, we observed the normal wood specific pectin methylesterase (CoPME) localization in differentiating xylem tracheids by immunolabeling. Labels localized at the entire perimeter of the compound middle lamella in normal wood, whereas sparse labeling was found in compression wood. It suggests that cell walls adhere at sites of CoPME function in differentiating xylem tracheids, but there is inadequate adhesion between cell walls where CoPME does not function. At the end of the expansion zone, the volume of the cell decreases due to a decrease in the turgor pressure of the tracheid. Further, due to moisture shrinkage of the tracheid, the adhesion begins to peel off in places of inadequate adhesion between cell walls, resulting in cell gaps and, thereby, generating a circular cell shape of cell wall formation in compression wood.

Keywords

Reaction Wood, Wood Formation, Cell Differentiation, Immunohistochemistry, Quantitative Polymerase Chain Reaction, Monoclonal Antibody

1. Introduction

To support inclined stems and branches, trees form specific secondary xylems called "reaction wood" in tissue morphology and physical property [1] [2]. Reaction wood for coniferous trees is called "compression wood", and they are formed on the lower sides of inclined stems and branches [2] [3] [4] [5] [6]. The formed compression wood generates large growth stress in the axial direction and bends the stem and branches growing due to growth stress to push the tree upward [7] [8]. Compression wood has different anatomical and chemical properties than normal wood [5] [6]. The main feature of compression wood is as follows: lower cellulose content and higher lignin content than normal wood, thick S1 layer, absent S3 layer, and reddish-brown color on wood surface. Furthermore, while transverse sections of normal wood tracheids forming in the vertical stems tend to have cell walls adhering to each other, the transverse sections of compression wood tracheids are circular and have intercellular spaces [3] [4] [5] [6] [9]. In this study, we attempted to elucidate the cause of compression wood tracheids becoming circular.

Intercellular adhesion in plant cells occurs via the cell wall. We examined factors involved in adhesion between cell walls and focused on the cell wall polysaccharide pectin, which plays an important role in intercellular adhesion. Pectin is the major constituent of the middle lamella and primary cell wall of plant cell walls [10] [11] [12], and it is a complex polysaccharide formed by the linking of three major structural regions of homogalacturonan (HG), rhamnogalacturonan-I (RG-I), and rhamnogalacturonan-II (RG-II) [12] [13] [14] [15]. Of the pectin constituent regions, homogalacturonan is extensively methyl esterified (80% - 90%) during the biosynthesis process, and it accumulates on the cell wall [11] [16] [17] [18]. Subsequently, the hydrolytic enzyme pectin methylesterase (PME, EC 3.1.1.11, CAZy CE8) catalyzes demethylation of the methyl group of homogalacturonan in the cell wall. This process releases methanol and a proton, thereby making the carboxyl group of homogalacturonan negatively charged [12] [19]. In the demethylated homogalacturonan, the negatively charged carboxyl group and Ca^{2+} ions are cross-linked [17] [20]. This then promotes formation of a model structure called the "egg box" between molecules [21] [22] [23], forming a pectin gel that acts as an adhesive [12] [18] [24] [25] and hardens the cell wall [17] [20] [24]. Pectin is believed to be involved in adhesion between cell walls through this process.

Observation of transverse sections of differentiating xylem tracheids of com-

pression wood with freeze fixation method have shown cell walls to adhere to one another between the cambium to expansion zone. Afterwards, when lignification begins, the adhesive peels off at the cell corner, and intercellular spaces appear. Finally, once lignification is complete, the transverse section of the tracheid shows a circular shape. Although, using chemical fixation method, the cell already become round shape in expansion zone. In order to understand how pectin methylesterase is involved in the transverse section of the tracheid during the cell wall formation process, it is necessary to know the time and locality in which pectin methylesterase functions. We first quantified the expression level of the pectin methylesterase gene in differentiating xylem cells of *Chamaecyparis obtusa* (Siebold & Zucc.) Endl. by quantitative real-time PCR, using different degrees of compression wood samples, and then investigated in each sample how PME gene expression correlated with the circularity of the transverse section of the tracheid. We prepared compression wood samples with different degrees of development by varying the tilt angle of the stem. Furthermore, through immunohistochemical staining, we examined the localization of normal wood specific pectin methylesterase (CoPME) and homogalacturonan in the differentiating xylem tracheids of *Chamaecyparis obtusa*. To examine the localization of CoPME, we created an antibody that specifically binds CoPME in the differentiating xylem of *Chamaecyparis obtusa.* Furthermore, to examine the localization of homogalacturonan, we used two types of monoclonal antibodies (LM19, LM20). They recognize different degrees of methyl esterification on homogalacturonan. LM20 recognizes highly and partially methyl-esterified (highly methylated) homogalacturonan, which is a substrate for PME. LM19 recognizes partially methyl-esterified and un-esterified (low methylated) homogalacturonan, which is a product of PME [26]. In this paper, we discuss the validity of CoPME being involved in the circularity of transverse sections of compression wood tracheid.

2. Materials and Methods

2.1. Plant Material

Samples for quantitative real-time PCR (qPCR) were grown from April to June 2015 in a field owned by Nagoya University, Japan. Twenty Japanese cypress (*C. obtusa*) saplings (about 100 cm in height) were planted in plastic pots filled with a mixture of red soil and compost. The saplings were loosely fixed to a stake using wire to maintain vertical stem growth. Four of these saplings were grown vertically to generate normal wood. In order to prepare compression wood of different levels of development, we grew 16 other saplings, with four saplings each being grown at four different tilt angles (5˚, 10˚, 20˚, and 30˚). Sampling was conducted during the most active period of cambial growth in June. After removing the bark, the stems of the saplings were cut into segments and the differentiating xylem tissues in the cut portions were harvested using a chisel. The lower sides of the stems (compression wood) were collected from the inclined

saplings, and both sides of the stems were collected from the vertical saplings (normal wood). Immediately after harvesting, these tissues were frozen in liquid nitrogen and stored at −80˚C for total RNA extraction. We also prepared samples to be used for tissue observations for measuring circularity of the transverse section of the xylem tracheid. After harvesting the differentiating xylem for total RNA extraction, we sampled the stem by using a saw to cut the surface where the tilt angle of the stem was constant in each sapling.

Samples for immunolabeling and protein extraction were grown from April to June 2016. Twenty Japanese cypress (*C. obtusa*) saplings (about 100 cm in height) were grown at the same condition of a previous experiment. Eight of these saplings were grown at an angle (*i.e.* with non-vertical stems) to generate compression wood. The other twelve saplings were grown vertically to generate normal wood. Each of the saplings with compression/normal wood was used for immunolabeling. Selected pieces of stem that included differentiating compression/normal wood were harvested from the saplings and cut with a razor blade into small square blocks measuring several millimeters on each side. The other saplings with compression/normal wood were used for protein extraction. The differentiating xylem tissues were collected using the same harvesting method for total RNA extraction. Immediately after harvesting, these tissues were frozen in liquid nitrogen and stored at −80˚C for protein extraction.

2.2. Quantitative Real-Time PCR (qPCR)

Total RNA was extracted from 50 mg of differentiating xylem sample using an RNeasy Plant Mini Kit (Qiagen, Valencia, CA, USA) according to the manufacturer's protocol. The RNA concentration was estimated spectrophotometrically using Gene Quant (Amersham, Buckinghamshire, UK). The RNA samples were treated with DNase I (TaKaRa Bio, Otsu, Japan) to remove contaminating genomic DNA. The removal of genomic DNA was confirmed by agarose gel electrophoresis after PCR amplification of 5 ng of the RNA samples. Total RNA was converted into cDNA using PrimeScript RT Master Mix (TaKaRa Bio). The cDNA products were used as a template in the qPCR. Based on the contig sequence homologous to the PME gene obtained by analysis of gene expression using a next-generation sequencer [27], gene-specific primers were designed using Primer 3 Plus (http://www.bioinformatics.nl/cgi-bin/primer3plus/primer3plus.cgi/) [28]. The primer sequences were as follows: Hinoki_PME_F, 5'-TGTCAGAGCCAGTGAAGAGAGAG-3'; Hinoki_PME_R, 5'-ATCGCCACAAACACAAGGAG-3'. The quantitative reaction was performed on a StepOnePlus Real Time PCR System (Life Technologies, Carlsbad, CA, USA) using the POWER SYBR Green PCR Master Mix (Life Technologies). The reaction mixture (20 μL) contained 2× POWER SYBR Master Mix, 0.2 μM each of the forward and reverse primers, and 5 ng of template cDNA. PCR amplification was performed under the following conditions: 95˚C

for 10 min, followed by 40 cycles at 95˚C for 15 s and 58˚C for 60 s and was performed three times per sample. Gene expression was normalized against ubiquitin as an endogenous gene [27] [29]. Relative gene expression was calculated using the comparative CT method [30].

2.3. Circularity Measurement of Xylem Tracheid Transverse Sections

Harvested stem segments were fixed in 3% glutaraldehyde in 67 mM phosphate buffer (pH 7.0) for 1 week at 4˚C. Subsequently, fixation in phosphate buffer was repeated. Transverse sections, 10 μm thick, were prepared from the segments using a sliding microtome. The sections were stained with 1% safranin and dehydrated in an increasing ethanol series. After soaking in xylene, the sections were mounted on glass slides with EntellanNeu (Merck, Darmstadt, Germany) and observed under a light microscope (BX60; Olympus, Tokyo, Japan). The observations were captured using a camera (DP70; Olympus, 1360 × 1024 pixels). Ten cells were selected for each sample, and the area and the perimeter of the intracellular cavity of the transverse section of the xylem tracheid were measured using the image processing software ImageJ. Following, the circularity (R) was calculated. Circularity is a parameter showing how close a shape is to a circle, and as circularity approaches 1, the closer a shape is to a true circle. Circularity is defined by the following formula:

$$R = \frac{4\pi S}{L^2}$$

(S is area, L is the perimeter).

2.4. Determination of CoPME gene Base Sequence

To create the anti-PME antibody, we used cDNA cloning and sequencing to identify the accurate base sequence of the PME gene that was expressed in differentiating xylem cells. The reverse transcribed cDNA of total RNA obtained from differentiating xylem cells of *C. obtusa* normal wood was amplified by PCR. Primers to amplify the Open Reading Frame (ORF) region of the contig sequence were designed using Primer 3 Plus. The primer sequences were as follows: Hinoki_PME_ORF_F, 5'-AATTAACGGCAAGCAAATCG-3'; Hinoki_PME_ORF_R, 5'-GAGTGCGCGAGTATTCCTTC-3'. We then amplified the ORF region using the primer pair and TaKaRa Ex Taq® Hot Start Version (TaKaRa). The amplified cDNA fragments were inserted into the pGEM-T Easy Vector (Promega, Madison, WI, USA) using T4 DNA Ligase, and their sequences were determined. The new sequences were submitted to the DNA Data Bank of Japan (Accession number: LC348962).

2.5. Protein Extraction

We grinded portions (5 - 10 g) of the differentiating xylem in liquid nitrogen to produce a powder. To obtain the soluble and ionically bound proteins, we ex-

tracted the differentiating xylem overnight in 50 mM sodium acetate-acetic acid buffer (pH 5.0) containing 1 M $CaCl_2$, polyvinyl pyrrolidone (3% of sample weight), 0.5 mM phenylmethylsulfonyl fluoride, and 5 mM β-mercaptoethanol at 4˚C. After extraction, the buffer was exchanged with 50 mM sodium acetate-acetic acid buffer (pH 5.0) by dialysis. The protein was concentrated using a Vivaspin 20 sample concentrator (GE Healthcare, Buckinghamshire, UK).

We determined protein concentrations by the Bradford procedure using bovine serum albumin (BSA) as the standard [31].

2.6. Western Blotting

Rabbit anti-PME immunoglobulin G (IgG) antibody was designed based on the amino acid sequence of the PME protein (ASEGSNGNEN); the peptide of this amino acid sequence was used as the antigen to raise the rabbit IgG antibody. To absorb the anti-PME antibody into the antigen, we mixed the anti-PME antibody and antigen (peptide of ASEGSNGNEN). Following, we incubated the mixture at 4˚C for 2 days. The proteins extracted from the differentiating xylem were separated by sodium dodecyl sulfate-PAGE (SDS-PAGE) (10%) and transferred to a polyvinylidine difluoride membrane (Fluorotrans W-F; Port Washington, NY, Pall Corporation). After washing the membrane in 20 mM Tris-HCl (TBS), pH 7.6, containing 0.1% (v/v) Tween 20 (TBS-T) buffer, we immersed it in TBS-T containing 2% (w/v) ECL Blocking reagent for 1 h at room temperature to block nonspecific antibody binding and washed in TBS-T. The membrane was immersed overnight in anti-PME antibody or absorbed anti-PME antibody diluted 100-fold with Can Get Signal Solution 1 (TOYOBO, Osaka, Japan) at 4˚C, and then washed thrice for 20 min in TBS-T. Subsequently, we immersed the membrane for 4 h in anti-rabbit IgG, HRP-linked whole Ab goat (MBL, Aichi, Japan) diluted 20,000-fold with Can Get Signal Solution 2 at room temperature and washed thrice for 20 min in TBS-T containing 0.5 M NaCl and 0.02% SDS. ECL Prime Western Blotting Detection Reagent (GE Healthcare) was used to generate chemiluminescence signals, which were detected with an LAS-1000 plus luminescent image analyzer (FUJIFILM, Tokyo, Japan).

2.7. Fixation and Embedding of Samples for Immunolabeling

Square stem blocks, each several millimeters on a side, were frozen rapidly by immersion in liquid chlorodifluoromethane (HCFC-22) cooled with liquid nitrogen. The blocks were transferred into an acetone solution containing 0.7% glutaraldehyde cooled to −80˚C, and then incubated for > 3 days to obtain a frozen substitute. The blocks were incubated at −20˚C overnight, then at 4˚C overnight. After equilibrating the blocks to room temperature, we immediately washed them thrice for 10 min in acetone. Subsequently, the block was immersed thrice for 1 h in 100% ethanol to replace acetone with ethanol. After this, the block was immersed overnight in a solution of ethanol:LR White resin = 1:1.

They were embedded in LR White resin (London Resin Co., Basingstoke, UK). The resin was cured at 50˚C overnight in airtight gelatin capsules.

2.8. Immunolabeling

Immunolabelling was conducted according to procedures described previously [32] [33]. Transverse thin (0.5 μm) sections for immunofluorescence light microscopy were cut using a rotary microtome (HM 350; MICROM, Walldorf, Germany) with a diamond knife and then mounted on MAS-GP typeA slides (Matsunami, Osaka, Japan). Each section was first immersed in 1% (w/v) BSA/TBS-T for 1 h to block nonspecific binding. The sections were then washed thrice for 15 min in TBS-T.

The anti-PME antibody used for western blotting was employed for immunolabeling. Each section was incubated in the anti-PME antibody diluted 10-fold in 1% BSA/TBS-T at 4˚C for 2 days, then washed thrice for 15 min in TBS-T. The sections were incubated in the goat anti-rabbit IgG secondary antibody, Alexa Fluor 647 (Thermo Fisher Scientific, MA, USA) diluted 300-fold in 1% BSA/TBS-T at 35˚C for 4 h. We shaded the sections from light during and after this treatment. The sections were washed thrice for 15 min in TBS-T and mounted in Fluoromount/Plus medium (Diagnostic BioSystems, CA, USA). We detected Alexa 647 fluorescence in the sections by confocal laser scanning microscopy (Fluoview FV10i; Olympus, Tokyo, Japan). Controls were prepared by replacing with 1) 1% BSA/TBS-T or 2) solutions of the anti-PME antibody absorbed into the antigen (diluted 10-fold).

The monoclonal antibodies LM19, LM20 (PlantProbes, Leeds, UK) were also employed for immunolabeling of homogalacturonans. Each section was incubated in LM19 or LM20 diluted 10-fold in 1% BSA/TBS-T for 2 days at 4˚C, then washed thrice for 15 min in TBS-T. The sections were incubated in the goat anti-rat IgM secondary antibody, Alexa Fluor 647 (Thermo Fisher Scientific) diluted 100-fold in 1% BSA/TBS-T at 35˚C for 4 h. The subsequent procedure was similar to the immunolabeling procedure of the anti-PME antibody. Controls were prepared by replacing with 1) 1% BSA/TBS-T or 2) solutions of the LM19 and LM20 absorbed into their respective antigens (LM19 diluted 10-fold in a solution of 1 mg of polygalacturonic acid per mL, LM20 diluted 10-fold in a solution of 1 mg of pectin per mL) [34].

3. Results

3.1. Relationship between Circularity and Gene Expression Level in Transverse Sections of Differentiating Xylem Tracheid

We measured the circularity of transverse sections of differentiating xylem tracheid in samples grown at five different tilt angles of the stem. As a result, we observed circularity in transverse sections of the tracheid, which is characteristic of compression wood, in samples from stem tilt angle greater than 10˚ (**Figure 1(c)-(e)**). Circularity of transverse sections of the xylem tracheid increased with

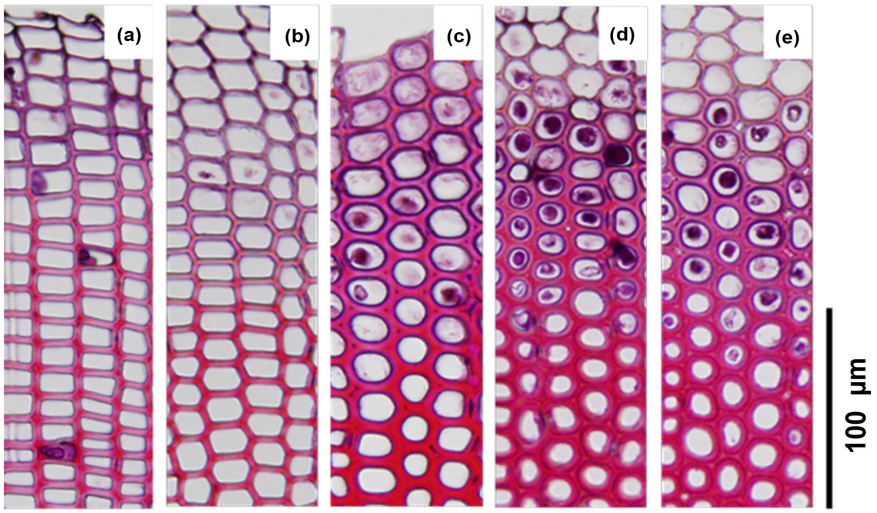

Figure 1. Image of transverse section of *C. obtusa*xylem tracheid. Safranin staining shows lignin in the cell wall (red). (a) Vertically grown sapling; (b) Sapling grown at a tilt angle of 5˚C; (c) Sapling grown at a tilt angle of 10˚; (d) Sapling grown at a tilt angle of 20˚; (e) Sapling grown at a tilt angel of 30˚

greater tilt angles of the stem. For each sample, we then compared the PME gene expression level in differentiating xylem cells quantified by quantitative real-time PCR and the circularity of the transverse section of the xylem tracheid. The results showed greater circularity of the transverse section of the xylem tracheid for samples with relatively low level of PME gene expression (**Figure 2**). For samples with average circularity near 0.95, *i.e.* samples with circular transverse sections of the xylem tracheid, the relative level of PME gene expression was less than 1/10 of that observed in samples with a square-shaped transverse section of the xylem tracheid.

3.2. Western Blotting

To determine whether the anti-CoPME antibody could specifically recognize the *C. obtusa* PME, we performed western blotting of the anti-CoPME antibody against proteins extracted fro/m the differentiating xylem of normal and compression wood. The anti-CoPME antibody reacted to proteins extracted from differentiating xylem of *C. obtusa*. We detected two signals from proteins extracted from normal wood (**Figure 3(a)**). A strong signal was seen in the molecular weight range of 55 and 60 kDa, while a weak signal was observed between 37 and 39 kDa. Similar results were observed from proteins extracted from compression wood (**Figure 3(b)**). However, the anti-CoPME antibody absorbed by antigen did not react to proteins extracted from the differentiating xylem of *C. obtusa* (**Figure 3(a)**, **Figure 3(b)**).

3.3. Immunolocalization of PME in Differentiating Xylem Tracheid Using Anti-CoPME Antibody

The anti-CoPME antibody was used for immunolabeling to observe the transverse

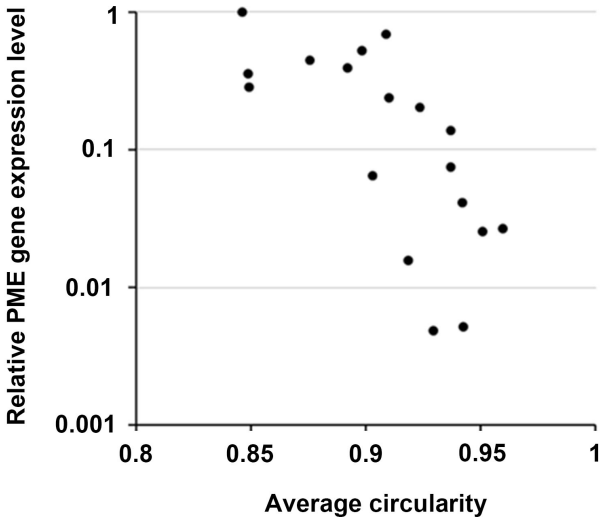

Figure 2. Relationship between relative PME gene expression level and average circularity in *C. obtuse* differentiating xylem cells. Relative to the gene expression level of 1 in a certain sample, gene expression levels in other samples are shown. For circularity, the circularity of 10 cells was measured for each sample before showing an average value. For example, the circularity was 0.785 for a square, 0.9 for a hexagon, and 1.0 for a circle.

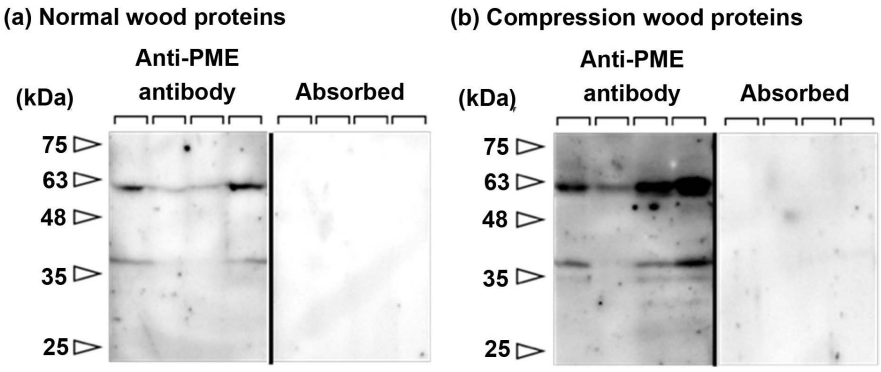

Figure 3. Specificity of the anti-PME antibody by Western blotting. (a) Reaction of proteins from normal wood with the anti-PME detected one strong signal and one weak signal (four lanes on the left side). Reaction with anti-PME antibody absorbed with antigen did not produce signals (four lanes on the right side); (b) Similar results of proteins from normal wood were obtained from compression wood proteins reacted with anti-PME antibody (four lanes on the left side) and anti-PME antibody absorbed with antigen (four lanes on the right side).

section of differentiating xylem tracheid from the cambium to the xylem tracheid. In sections of normal wood, labeling was seen in the compound middle lamella from the cambium to the expansion zone (**Figure 4(b)**). There was labeling across the entire perimeter of the cell wall after the expansion zone ended and thickening of the secondary wall started. There was also labeling in the cell corner. Furthermore, in sections of compression wood, there was sparse labeling on the cell walls from the cambium to the mature cell (**Figure 5(b)**). From the

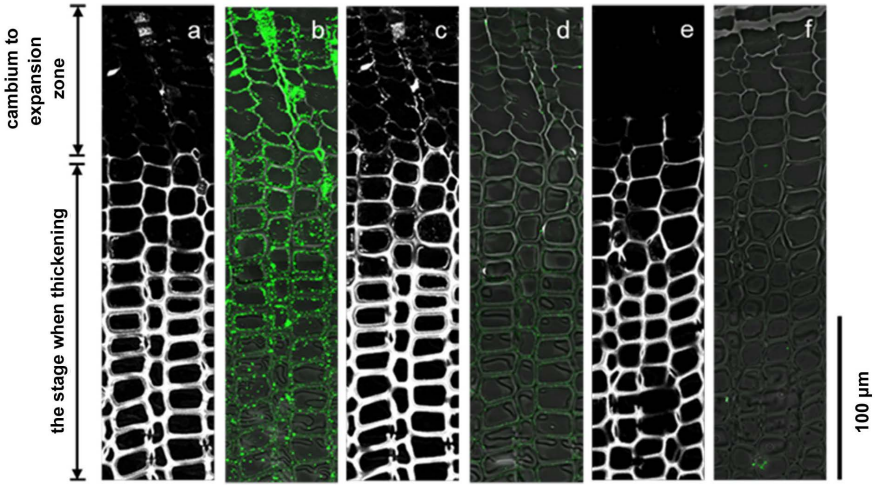

Figure 4. Immunolabeling images of the transverse sections of normal wood differentiating xylem tracheid using anti-PME antibody. Image (a) and image (b), image (c) and image (d), and image e and image (f) show the same sections. (a), (c), and (e) are images of lignin autofluorescence excited at 488 nm wavelength (white). (b) Overlapping phase-contrast image of the anti-PME antibody labeled image (green). (d) Overlapping phase-contrast image of the anti-PME antibody absorbed with antigen labeled image (green). (f) Overlapping phase-contrast image of the labeled image of proteins reacting without the anti-PME antibody (control, green).

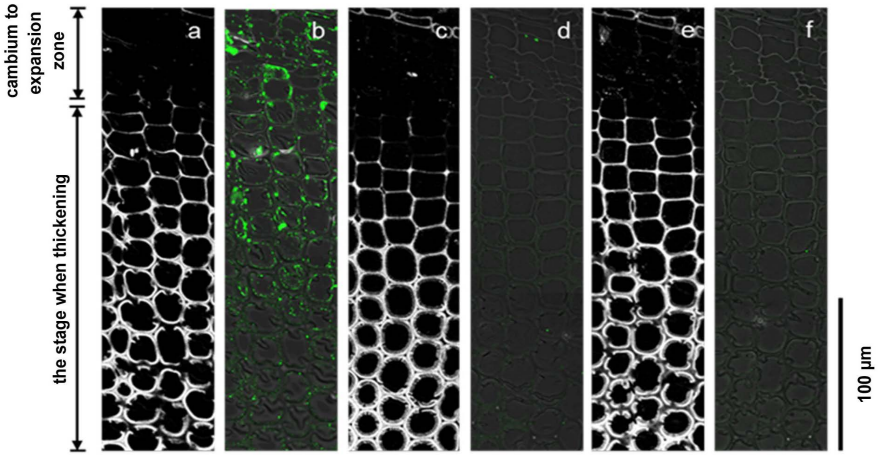

Figure 5. Immunolabeling images of the transverse sections of compression wood differentiating xylem tracheid using anti-PME antibody. Images (a) and (b), images (c) and (d), and images (e) and (f) show the same sections. (a), (c), and (e) are images of lignin autofluorescence excited at 488 nm wavelength (white). (b) Overlapping phase-contrast image of the anti-PME antibody labeled image (green). (d) Overlapping phase-contrast image of the anti-PME antibody absorbed with antigen labeled image (green). (f) Overlapping phase-contrast image of the labeled image of proteins reacting without the anti-PME antibody (control, green).

cambium to the mature cell, the sections of normal wood showed more intense labeling than compression wood. In both types of sections, there was no labeling in the secondary wall at the stage when thickening was completed. When the anti-CoPME antibody absorbed with antigen was used as a control, there was no

labeling either in sections of normal wood or compression wood (Figure 4(d), Figure 5(d)). There was no labeling in either sections of normal wood or compression wood even when using a control with the anti-CoPME antibody removed (Figure 4(f), Figure 5(f)).

3.4. Immunolocalization of Homogalacturonan in Differentiating Xylem Tracheid Using LM19 and LM20 Antibodies

The anti-homogalacturonan antibodies LM19 and LM20 were used for immunolabeling to observe the transverse section of differentiating xylem tracheid from the cambium to the xylem tracheid. LM19 recognizes low methylated homogalacturonan, while LM20 recognizes highly methylated homogalacturonan. Observation of normal wood sections using the LM19 antibody showed labeling in the compound middle lamella from the cambium to the expansion zone (Figure 6(b)). There was particularly intense labeling in the radial wall. After the end of the expansion zone and start of the thickening of the secondary wall, labeling in the radial wall weakened, and there was no labeling in the tangential wall. No labeling was observed in the cell corner. There was no labeling in the secondary wall at the stage when thickening was completed. Furthermore, in compression wood sections, the middle lamella between the cambium and expansion zone showed weaker labeling than in sections of normal wood (Figure 7(b)). After the end of the expansion zone and start of thickening of the secondary wall, similar to normal wood sections, labeling in the radial wall weakened, while there was no labeling in the tangential wall of sections of compression wood. Using the LM19 antibody absorbed with 1 mg/mL polygalacturonic acid solution, neither normal wood nor compression wood sections showed labeling (Figure 6(d), Figure 7(d)).

When the LM20 antibody was used to observe normal wood sections, there was labeling in the middle lamella between the cambium and expansion zone (Figure 8(b)). There was particularly intense labeling in the radial wall. After the end of the expansion zone and start of the thickening of secondary wall, there was labeling in the radial wall, but labeling in the tangential wall had weakened. There was intense labeling in the cell corner. There was no labeling in the secondary wall at the stage when thickening had completed. Similar labeling patterns as normal wood sections were seen in compression wood sections (Figure 9(b)). Moreover, using the LM20 antibody absorbed with 1 mg/mL pectin solution, neither normal wood nor compression wood sections showed labeling (Figure 8(d), Figure 9(d)). Neither normal wood nor compression wood sections showed any labeling using a control that had LM19 and LM20 removed (Figure 6(f), Figure 7(f)).

4. Discussion

4.1. Relationship between Circularity in the Transverse Section of xylem Tracheid and Gene Expression Levels

The graph, which shows the relationship between relative PME gene expression

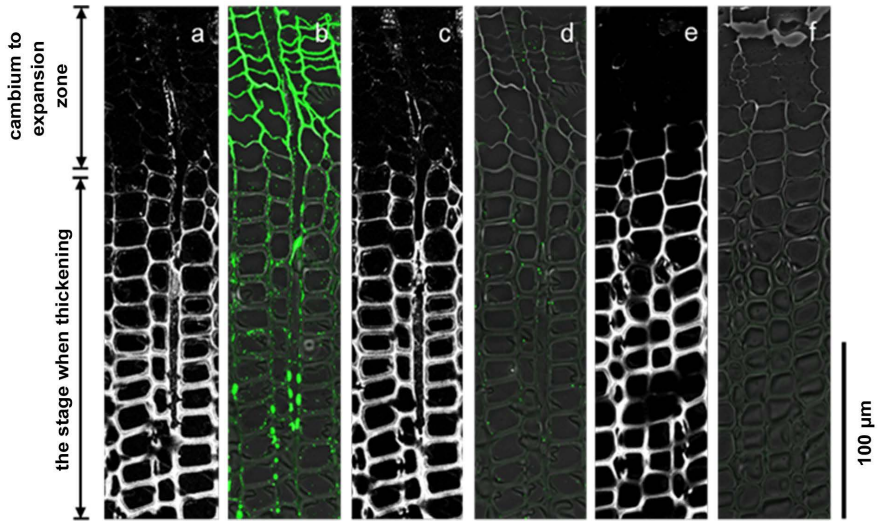

Figure 6. Immunolabeling images of the transverse sections of normal wood differentiating xylem tracheid using LM19 antibody (which recognizes low methylated homogalacturonan). Images (a) and (b), images (c) and (d), and images (e) and (f) show the same sections. (a), (c), and (e) are images of lignin autofluorescence excited at 488 nm wavelength (white); (b) Overlapping phase-contrast image of the LM19 antibody labeled image (green); (d) Overlapping phase-contrast image of the LM19 antibody absorbed with 1 mg/mL polygalacturonic acid solution labeled image (green); (f) Overlapping phase-contrast image of the labeled image of proteins reacting without the LM19 antibody (control, green).

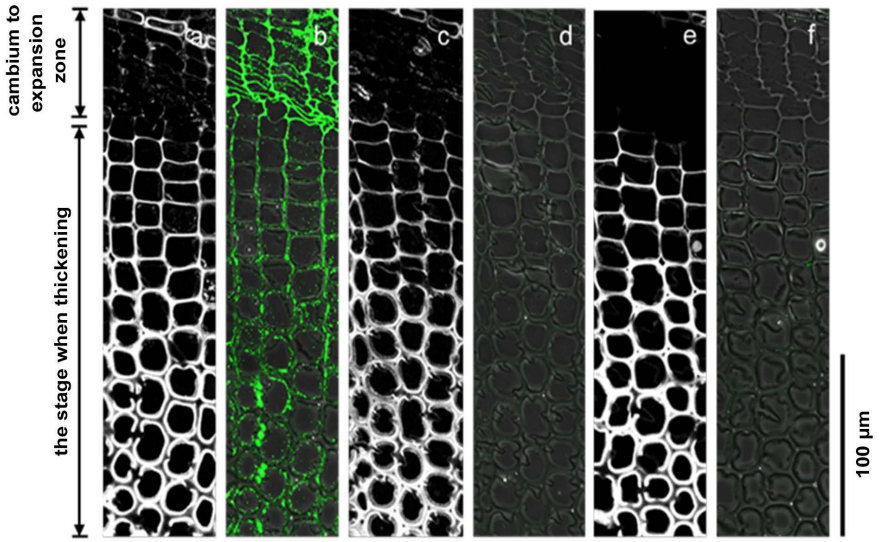

Figure 7. Immunolabeling images of the transverse sections of compression wood differentiating xylem tracheid using LM19 antibody (which recognizes low methylated homogalacturonan). Images (a) and (b), images (c) and (d), and images (e) and (f) show the same sections. (a), (c), and (e) are images of lignin autofluorescence excited at 488 nm wavelength (white). (b) Overlapping phase-contrast image of the LM19 antibody labeled image (green). (d) Overlapping phase-contrast image of the LM19 antibody absorbed with 1 mg/mL polygalacturonic acid solution labeled image (green). (f) Overlapping phase-contrast image of the labeled image of proteins reacting without the LM19 antibody (control, green).

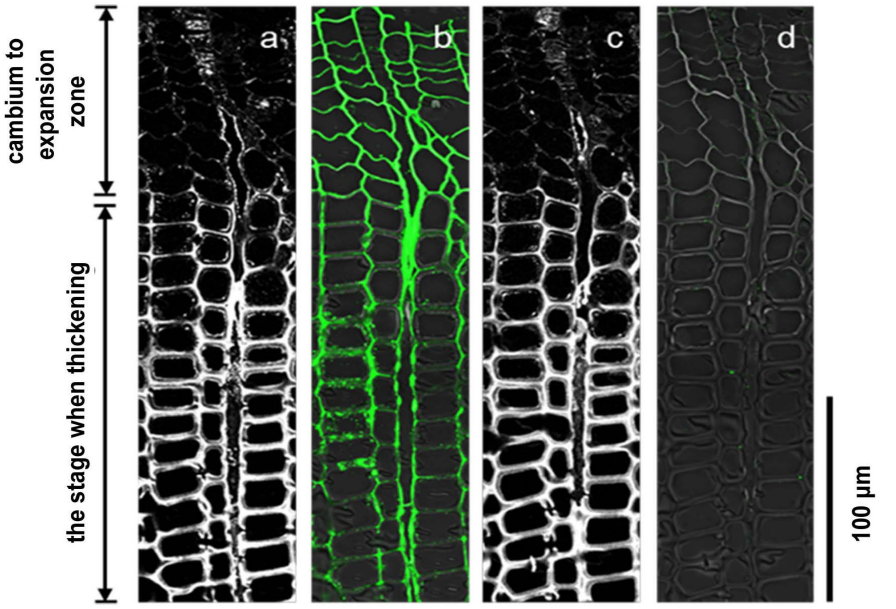

Figure 8. Immunolabeling images of the transverse sections of normal wood differentiating xylem tracheid using LM20 antibody (which recognizes highly methylated homogalacturonan). Images (a) and (b) and images (c) and (d) show the same sections. (a). and (c) are images of lignin autofluorescence excited at 488 nm wavelength (white). (b) Overlapping phase-contrast image of the LM20 antibody labeled image (green). (d) Overlapping phase-contrast image of the LM20 antibody absorbed with 1 mg/mL pectin solution labeled image (green).

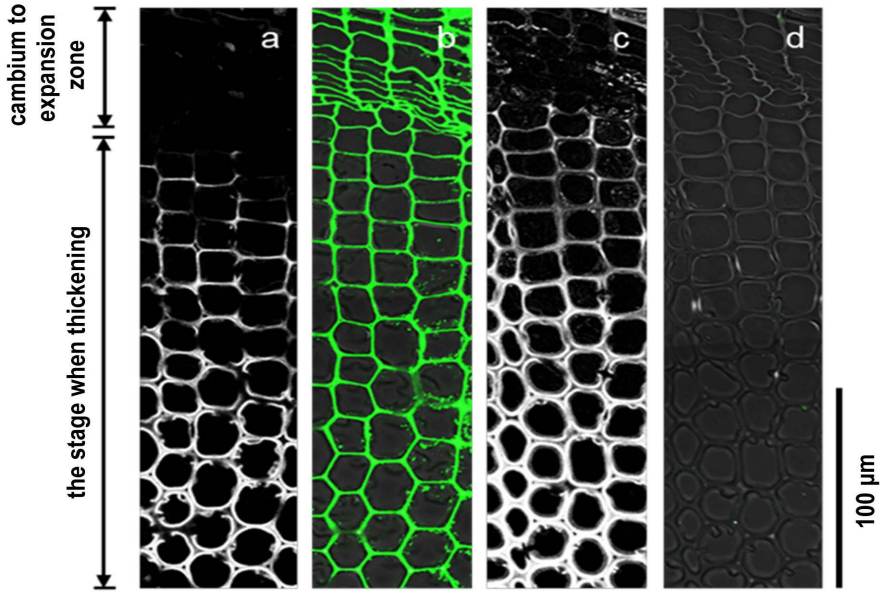

Figure 9. Immunolabeling images of the transverse sections of compression wood differentiating xylem tracheid using LM20 antibody (which recognizes highly methylated homogalacturonan). Images (a) and (b) and images (c) and (d) show the same sections. (a) and (c) are images of lignin autofluorescence excited at 488 nm wavelength (white). (b) Overlapping phase-contrast image of the LM20 antibody labeled image (green). (d) Overlapping phase-contrast image of the LM20 antibody absorbed with 1 mg/mL pectin solution labeled image (green).

level in *C. obtusa* differentiating xylem cells and the average circularity of the transverse section of xylem tracheid, indicated that lower PME gene expression levels are correlated to greater circularity of the transverse section of the xylem tracheid. Therefore, circularity of the transverse section of xylem tracheid may be caused by expressional inhibition of the PME gene. In this study, we have quantified the gene expression levels by sampling differentiating xylem cells from the region between the cambium to the expansion zone. For this reason, we believe that expression of the PME gene may have been suppressed prior to circularity of the transverse sections of the tracheid.

4.2. Test of the Anti-CoPME Antibody Specificity

We used Western blotting to test the specificity of the anti-CoPME antibody. In the normal wood sample and compression wood sample, we detected a strong signal near molecular weights of 55 - 0 kDa. We converted the cDNA sequence of the PME gene functioning in the differentiating xylem, obtained by sequencing, to an amino acid sequence and analyzed the sequence using the EXPazy-ProtParam tool (https://web.expasy.org/protparam/). This revealed that the total molecular weight of this protein was at least 53 kDa. Therefore, this suggests that the anti-CoPME antibody may have recognized and bound to the PME present in the differentiating xylem.

Furthermore, in both the normal wood sample and compression wood sample, we detected a signal near molecular weights of 37 - 39 kDa. We believe that this signal recognized the PME cleaved at a certain site in the amino acid region by proteases. However, it is also possible that the anti-CoPME antibody is non-specifically bound to a different protein with a similar sequence to the peptide sequence (ASEGSNGNEN). In order to identify the protein detected by the anti-CoPME antibody, it is necessary to recover the protein bound to the anti-CoPME antibody and investigate the amino acid sequence of said protein. However, anti-CoPME antibody absorbed by antigen did not recognize any protein extracted from the differentiating xylem. For this reason, we believe that the signal detected was due to recognition of PME present in the differentiating xylem by the anti-CoPME antibody.

4.3. Localization of CoPME in the Differentiating Xylem Tracheids

Through immunolabeling using the anti-CoPME antibody, we examined CoPME localization in transverse sections of the differentiating xylem tracheids. CoPME labeling was observed in the compound middle lamella between the cambium and expansion zone in sections of normal wood and compression wood. Labeling was also mainly observed in the compound middle lamella, from the expansion zone to the mature cell. As a result, we inferred that CoPME was present in the compound middle lamella between the cambium and mature cells. It has been shown that in the differentiating xylem of *Populus euramerica* branches, PME is present in the compound middle lamella of the radial wall and in the cell corner [35]. This

study produced similar results. When immunolabeling was carried out using anti-CoPME absorbed with antigen, there was no labeling. Therefore, we believe that the labeling indicated CoPME recognition present in the differentiating xylem tracheids by the anti-CoPME antibody.

4.4. Localization of Homogalacturonan in the Differentiating Xylem Tracheids

Through immunolabeling using the anti-homogalacturonan antibodies LM19 and LM20, we examined homogalacturonan localization in transverse sections of the differentiating xylem tracheids. LM20 recognizes highly methylated homogalacturonan, which serves as a substrate when PME is functioning. LM19 recognizes low methylated homogalacturonan, which is produced when PME functions.

LM20 labeling was observed in compound middle lamella between the cambium and expansion zone, in both normal wood and compression wood sections. Labeling was also observed in compound middle lamella of the radial wall, from the expansion zone to the mature cell. This result suggested that highly methylated homogalacturonan, which is the substrate when PME is functioning, is present in abundance in the compound middle lamella between the cambium and mature cell. In the differentiating xylem of *Populus euramerica* branches, highly methylated homogalacturonan is reportedly present in the middle lamella of the radial wall and tangential wall in the cambium [34] [36], and similar results were observed in this study. No labeling was observed when immunolabeling was performed using the LM20 antibody absorbed with pectin solution. Therefore, we believe that labeling showed recognition of highly methylated homogalacturonan present in the differentiating xylem tracheids by the LM20 antibody.

LM19 labeling was observed in compound middle lamella between the cambium and expansion zone in both normal wood and compression wood sections. The intensity of labeling weakened from the expansion zone to the mature cell. In the differentiating xylem of *Populus euramerica* branches, low methylated homogalacturonan is reportedly weakened significantly as the secondary wall was thickening, and similar results were observed in this study [36]. LM19 antibody may not have recognized the low methylated homogalacturonan, which composed the pectin gel that functions as an adhesive between cell walls. In the differentiating xylem of *Populus euramerica* branches, low methylated homogalacturonan is reportedly present in the intermediate layer of the radial wall in the cambium [34], but this study did not produce similar results. No labeling was observed when immunolabeling was performed using the LM19 antibody absorbed with polygalacturonic acid solution. Therefore, we believe that labeling indicated recognition of low methylated homogalacturonan present in the differentiating xylem tracheids by the LM19 antibody.

It is also conceivable that highly methylated homogalacturonan is present in greater quantity than low methylated homogalacturonan in the cell walls of ma-

ture cells. In mature cells, highly methylated homogalacturonan may be the majority form of homogalacturonan present, and low methylated homogalacturonan may only be present in small amounts. However, the result in this study, in which far more labeling of highly methylated homogalacturonan than low methylated homogalacturonan in the compound middle lamella was found, was similar to the observations made from immunohistochemical staining of homogalacturonan in mature xylem of *Pinus sylvestris* [37]. Several hypotheses have been proposed to explain the greater amount of highly methylated homogalacturonan than low methylated homogalacturonan in cell walls after lignification. It has been reported that the presence of Ca^{2+}, which is said to crosslink the carboxyl groups in low methylated homogalacturonan, causes one-electron oxidation of coniferyl alcohol and is involved in the lignification process [38]. In other words, the liberation of Ca^{2+} from homogalacturonan might be necessary for lignification to start after the end of the expansion zone. It has also been reported that in the presence of Ca^{2+}, low methylated homogalacturonan has affinity to isoperoxidase, which is responsible for polymerization of lignin [39]. These reports suggested that liberated Ca^{2+} and low methylated homogalacturonan may be involved in lignification of the cell wall.

4.5. Difference in Localization of CoPME between Tracheid of Normal Wood and Compression Wood

When the distribution of localized CoPME was compared between normal wood and compression wood sections, we observed that normal wood had more intense labeling than compression wood in the compound middle lamella from the cambium to expansion zone. This result suggested that the amount of CoPME present in the differentiating xylem of normal wood was greater than compression wood. This result also supports the relationship between increased circularity of transverse sections of the tracheid and decreased PME expression levels in

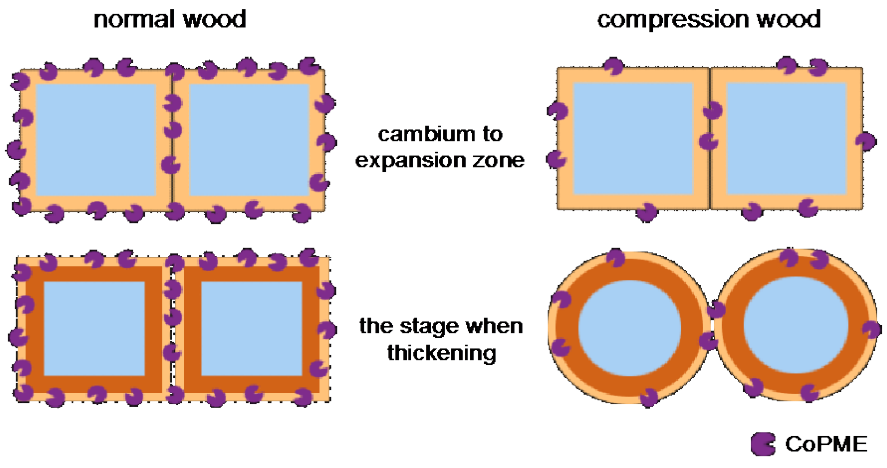

Figure 10. Schema for the hypothesis of generating a circular cell shape. In normal wood, CoPME labels localized at the entire perimeter of the compound middle lamella. In compression wood, their labels localized at sparse on the cell walls. It suggested that cell walls adhere at sites of CoPME function in differentiating xylem tracheids.

differentiating xylem cells. Further, we observed labeling around the entire perimeter of the cell wall in normal wood sections. Conversely, compression wood sections did not show labeling around the perimeter of the cell wall and, instead, showed sparse labeling. This result suggested that while CoPME was present all around the cell wall of normal wood, the same was not true for compression wood. We believe that cell shape becomes circular according to the following process of cell wall formation in compression wood. In places where CoPME functions, pectin gel formation allows sufficient adhesion between cell walls. However, in places where CoPME does not function, we believe that there is inadequate adhesion between cell walls. At the end of the expansion zone, the volume of the cell decreases due to a decrease in the turgor pressure of the tracheid. Further, due to moisture shrinkage of the tracheid, the adhesion begins to peel off in places of inadequate adhesion between cell walls, resulting in cell gaps and, thereby, generating a circular cell shape (**Figure 10**).

Acknowledgements

This work was supported by JSPS KAKENHI Grant Number JP17K19286.

Conflicts of Interest

The authors declare no conflicts of interest regarding the publication of this paper.

References

[1] Scurfield, G. (1973) Reaction Wood: Its Structure and Function. *Science*, **179**, 647-655. https://doi.org/10.1126/science.179.4074.647

[2] Wilson, B.F. and Archer, R.R. (1979) Tree Design: Some Biological Solutions to Mechanical Problems. *Bioscience*, **29**, 293-298. https://doi.org/10.2307/1307825

[3] Westing, A.H. (1965) Formation and Function of Compression Wood in Gymnosperms. *The Botanical Review*, **31**, 381-480. https://doi.org/10.1007/BF02859131

[4] Brown, C.L. (1971) Secondary Growth. In: Brown, C.L. and Zimmermann, M.H., Eds., *Tree*: *Structure and Function*, Springer-Verlag, Berlin, 98-99. https://doi.org/10.1007/978-3-642-88528-0_2

[5] Wilson, B.F. and Archer, R.R. (1977) Reaction Wood: Induction and Mechanical Action. *Annual Review of Plant Physiology*, **28**, 23-43. https://doi.org/10.1146/annurev.pp.28.060177.000323

[6] Timell, T.E. (1986) Compression Wood in Gymnosperms. Vol. 1, Springer, Berlin. https://doi.org/10.1007/978-3-642-61616-7_1

[7] Yamamoto, H., Okuyama, T., Yoshida, M. and Sugiyama, K. (1991) Generation Process of Growth Stresses in Cell Walls. III, *Mokuzai Gakkaishi*, **37**, 94-100.

[8] Yamamoto, H., Yoshida, M. and Okuyama, T. (2002) Growth Stress Controls Negative Gravitropism in Woody Plant Stems. *Planta*, **216**, 280-292. https://doi.org/10.1007/s00425-002-0846-x

[9] Côté, W.A. and Day, A.C. (1965) Anatomy and Ultrastructure of Reaction Wood. In: Côté, W.A., Ed., *Cellular Ultrastructure of Woody Plants*, Syracuse University Press, New York, 391-418.

[10] Bacic, A., Harris, P.J. and Stone, B.A. (1988) Structure and Function of Plant Cell Walls. In: Preiss, J., Ed., *The Biochemistry of Plants*, Vol. 14, Academic Press, New York, 297-371. https://doi.org/10.1016/B978-0-08-092615-5.50014-X

[11] O'Neill, M., Albersheim, P. and Darvill, A. (1990) The Pectic Polysaccharides of Primary Cell Walls. In: Dey, P.M., Ed., *Methods in Plant Biochemistry*, Vol. 2, Academic Press, New York, 415-441. https://doi.org/10.1016/B978-0-12-461012-5.50018-5

[12] Pelloux, J., Rustérucci, C. and Mellerowicz, E.J. (2007) New Insights into Pectin Meth-Ylesterase Structure and Function. *Trends in Plant Science*, **12**, 267-277. https://doi.org/10.1016/j.tplants.2007.04.001

[13] McCann, M.C. and Roberts, K. (1994) Changes in Cell Wall Architecture during Cell Elongation. *Journal of Experimental Botany*, **45**, 1683-1691. https://doi.org/10.1093/jxb/45.Special_Issue.1683

[14] Pérez, S., Mazeau, K. and Hervé du Penhoat, C. (2000) The Three-Dimensional Structures of the Pectic Polysaccharides. *Plant Physiology and Biochemistry*, **38**, 37-55. https://doi.org/10.1016/S0981-9428(00)00169-8

[15] Atmodjo, M.A., Hao, Z. and Mohnen, D. (2013) Evolving Views of Pectin Biosynthesis. *Annual Review of Plant Biology*, **64**, 747-779. https://doi.org/10.1146/annurev-arplant-042811-105534

[16] Zhang, G.F. and Staehelin, L.A. (1992) Functional Compartmentation of the Golgi Apparatus of Plant Cells. *Plant Physiology*, **99**, 1070-1083. https://doi.org/10.1104/pp.99.3.1070

[17] Micheli, F. (2001) Pectin Methylesterases: Cell Wall Enzymes with Important Roles in Plant Physiology. *Trends in Plant Science*, **6**, 414-419. https://doi.org/10.1016/S1360-1385(01)02045-3

[18] Daher, F.B. and Braybrook, S.A. (2015) How to Let Go: Pectin and Plant Cell Adhesion. *Frontiers in Plant Science*, **6**, 1-8. https://doi.org/10.3389/fpls.2015.00523

[19] Moustacas, A.M., Nari, J., Borel, M., Noat, G. and Ricard, J. (1991) Pectin Methylesterase, Metal Ions and Plant Cell-Wall Extension. The Role of Metal Ions in Plant Cell-Wall Extension. *Biochemical Journal*, **279**, 351-354. https://doi.org/10.1042/bj2790351

[20] Willats, W.G.T., Orfila, C., Limberg, G., Buchholt, H.C., Van Alebeek, G.J.W.M., Voragen, A.G.J., Marcus, S.E., Christensen, T.M.I.E., Mikkelsen, J.D., Murray, B.S. and Knox, J.P. (2001) Modulation of the Degree and Pattern of Methyl-Esterification of Pectic Homogalacturonan in Plant Cell Walls: Implications for Pectin Methyl Esterase Action, Matrix Properties, and Cell Adhesion. *The Journal of Biological Chemistry*, **276**, 19404-19413. https://doi.org/10.1074/jbc.M011242200

[21] Liners, F., Letesson, J.J., Didembourg, C. and Van Cutsem, P. (1989) Monoclonal Antibodies against Pectin: Recognition of a Conformation Induced by Calcium. *Plant Physiology*, **91**, 1419-1424. https://doi.org/10.1104/pp.91.4.1419

[22] Caffall, K.H. and Mohnen, D. (2009) The Structure, Function, and Biosynthesis of Plant Cell Wall Pectic Polysaccharides. *Carbohydrate Research*, **344**, 1879-1900. https://doi.org/10.1016/j.carres.2009.05.021

[23] Levesque-Tremblay, G., Pelloux, J., Braybrook, S.A. and Müller, K. (2015) Tuning of Pectin Methylesterification: Consequences for Cell Wall Biomechanics and Development. *Planta*, **242**, 791-811. https://doi.org/10.1007/s00425-015-2358-5

[24] Catesson, A.M. (1994) Cambial Ultrastructure and Biochemistry: Changes in Relation to Vascular Tissue Differentiation and the Seasonal Cycle. *International Journal of Plant Sciences*, **155**, 251-261. https://doi.org/10.1086/297165

[25] Goldberg, R., Morvan, C., Jauneau, A. and Jarvis, M.C. (1996) Methy-Esterification, De-Esterification and Gelation of Pectins in the Primary Cell Wall. *Progress in Biotechnology*, **14**, 151-172. https://doi.org/10.1016/S0921-0423(96)80253-X

[26] Verhertbruggen, Y., Marcus, S.E., Haeger, A., Ordaz-Ortiz, J.J. and Knox, J.P. (2009) An Extended Set of Monoclonal Antibodies to Pectic Homogalacturonan. *Carbohydrate Research*, **344**, 1858-1862. https://doi.org/10.1016/j.carres.2008.11.010

[27] Sato, S., Yoshida, M., Hiraide, H., Ihara, K. and Yamamoto, H. (2014) Transcriptome Analysis of Reaction Wood in Gymnosperms by Next-Generation Sequencing. *American Journal of Plant Sciences*, **5**, 2785-2798. https://doi.org/10.4236/ajps.2014.518295

[28] Untergasser, A., Nijveen, H., Rao, X., Bisseling, T., Geurts, R. and Leunissen, J.A.M. (2007) Primer3Plus, an Enhanced Web Interface to Primer3. *Nucleic Acids Research*, **35**, W71-W74. https://doi.org/10.1093/nar/gkm306

[29] Hiraide, H., Yoshida, M., Ihara, K., Sato, S. and Yamamoto, H. (2014) High Lignin Deposition on the Outer Region of the Secondary Wall Middle Layer in Compression Wood Matches the Expression of a Laccase Gene in *Chamaecyparis obtuse*. *Journal of Plant Biology Research*, **3**, 87-100.

[30] Livak, K.J. and Schmittgen, T.D. (2001) Analysis of Relative Gene Expression Data Using Real-Time Quantitative PCR and the 2(-Delta delta C(T)) Method. *Methods*, **25**, 402-408. https://doi.org/10.1006/meth.2001.1262

[31] Bradford, M.M. (1976) A Rapid and Sensitive Method for the Quantitation of Microgram Quantities of Protein Utilizing the Principle of Protein-Dye Binding. *Analytical Biochemistry*, **72**, 248-254. https://doi.org/10.1016/0003-2697(76)90527-3

[32] Hiraide, H., Yoshida, M., Sato, S. and Yamamoto, H. (2016) Common Mechanism of Lignification of Compression Wood in Conifers and Buxus. *American Journal of Plant Sciences*, **7**, 1151-1162. https://doi.org/10.4236/ajps.2016.77110

[33] Hiraide, H., Yoshida, M., Sato, S. and Yamamoto, H. (2016) *In Situ* Detection of Laccase Activity and Immunolocalisation of a Compression-Wood-Specific Laccase (CoLac1) in Differentiating Xylem of *Chamaecyparis obtusa*. *Functional Plant Biology*, **43**, 542-552. https://doi.org/10.1071/FP16044

[34] Guglielmino, N., Liberman, M., Jauneau, A., Vian, B., Catesson, A.M. and Goldberg, R. (1997) Pectin Immunolocalization and Calcium Visualization in Differentiating Derivatives from Poplar Cambium. *Protoplasma*, **199**, 151-160. https://doi.org/10.1007/BF01294503

[35] Guglielmino, N., Liberman, M., Catesson, A.M., Mareck, A., Prat, R., Mutaftschiev, S. and Goldberg, R. (1997) Pectin Methylesterases from Poplar Cambium and Inner Bark: Localization, Properties and Seasonal Changes. *Planta*, **202**, 70-75. https://doi.org/10.1007/s004250050104

[36] Liu, J., Hou, J., Chen, H., Pei, K., Li, Y. and He, X.Q. (2017) Dynamic Changes of Pectin Epitopes in Cell Walls during the Development of the Procambium-Cambium Continuum in Poplar. *International Journal of Molecular Sciences*, **18**, 1716. https://doi.org/10.3390/ijms18081716

[37] Hafrén, J., Daniel, G. and Westermark, U. (2000) The Distribution of Acidic and Esterified Pectin in Cambium, Developing Xylem and Mature Xylem of *Pinus sylvestris*. *Iawa Jouranal*, **21**, 157-168. https://doi.org/10.1163/22941932-90000242

[38] Westermark, U. (1982) Calcium Promoted Phenolic Coupling by Superoxide Radical: A Possible Lignification Reaction in Wood. *Wood Science and Technology*, **16**, 71-78. https://doi.org/10.1007/BF00351376

[39] Penel, C. and Greppin, H. (1994) Binding of Plant Isoperoxidases to Pectin in the Presence of Calcium. *FEBS Letters*, **343**, 51-55. https://doi.org/10.1016/0014-5793(94)80605-5